Supporting Information

Thiagarajan et al. 10.1073/pnas.1101026108

SI Text

Enzyme and Substrate Characterization from Steady State Absorption Spectra. Fig. S1*A* presents steady state UV-visible absorption spectra recorded at different stages of a typical transient absorption experiment at 266 nm. The corresponding spectra for a sample with a three times higher substrate concentration are shown in Fig. S1*B*. Our photolyase samples initially contained a mixture of $FADH^{\circ}$ and FAD_{ox} (main bands at 586 and 450 nm, respectively, in Fig. S1, black lines). These bands disappeared upon photoreduction (red lines), indicating virtually complete formation of $FADH^{-}$. After substrate addition (green lines) and subsequent transient absorption experiments using excitation flashes at 355 nm (blue lines), we observed only minor reoxidation to $FADH^{\circ}$ and FAD_{ox}.

The increase of the 265 nm absorption band upon flash excitation (from green to blue lines in Fig. S1) is a convenient measure for the amount of CPD repair. This increase was 35 mOD for Fig. S1*A* (8 μM substrate; 2.9 μM photolyase; 61 flashes of 1.16 mJ mean energy) and 24 mOD for Fig. S1*B* (24 μM substrate; 3.2 μM photolyase; 46 flashes of 1.05 mJ mean energy). Referred to photolyase concentration and total excitation energy, the 265-nm absorbance increase at 8 μM substrate (0.17 mOD per mJ and μM photolyase) and at 24 μM substrate (0.16 mOD per mJ and μM photolyase) were the same within precision of the experiment. Admitting an error margin of ±10% for each of the two experiments, it can be derived that the binding constant for our substrate is at least 8.5×10^5 M^{-1}. This value implies that under the conditions of our standard transient absorption experiments at 266 nm (approximately 10 μM substrate at 3.7 μM photolyase) at least 85% of the active enzymes had substrate bound. This number rises to at least 98% under the conditions of our standard transient absorption experiments in the visible (approximately 100 μM substrate at 37 μM photolyase). This does not rule out, however, that there may be a fraction of enzymes that do not bind substrate properly even at the large excess used in the visible.

Treatment of Original Transient Absorption Data. The signals presented in Fig. 2 and Fig. S2 are averages of several individually treated traces recorded on the digital oscilloscope. Voltage versus time traces were converted to absorbance change versus time traces $\Delta A(t)$ according to $\Delta A(t) = -\log(U(t)/U_0)$. $U(t)$ is the voltage recorded by the oscilloscope plus the DC level U_0 that would have been observed in a DC coupled amplification system prior to excitation. U_0 was obtained by multiplying the voltage measured at the side output of the bias-T by the amplification factor. Traces for which the excitation energy deviated by more than 15% from the average were discarded. As the internal clock of the oscilloscope was independent of the excitation laser, the temporal positions of the sampling points (every 25 ps) with respect to the external trigger signal (that was derived from the excitation flash and defined time zero of the oscilloscope) varied from one trace to another by up to ±12.5 ps. Before averaging, the individual traces were converted to traces with common sampling points by linear interpolation between the original data points. Afterwards, averaged signals from photolyase samples and from $[Ru(bpy)_3)]^{2+}$ recorded in the same series of experiments were together shifted in time such that the half rise of the $[Ru(bpy)_3)]^{2+}$ signal was at time zero. When averaged signals from different series of experiments had to be subtracted, common sampling points were created in the same way.

Quantification of CPD Repair After Transient Absorption Measurements at 266 nm. Before and after each set of transient absorption measurements (seven different measurements probing seven different volumes of the cell), a steady state absorption spectrum of the photolyase sample was recorded to determine the amount of T = T repaired by the seven excitation flashes from the increase of absorbance of the 265-nm band of intact thymine. This amount was generally consistent with the amount of repaired T = T estimated from the total absorption increase in the transient absorption measurements at 266 nm (see Fig. 2*D*, red trace), taking into account the dilution of the excited volume (approximately 20 μl) to the total volume (typically 300 μl).

Determination of the $[Ru(bpy)_3]^{2+*}$-minus-$[Ru(bpy)_3]^{2+}$ Differential Absorption Coefficients at the Monitoring Wavelengths Used in this Study. Several absorbance difference spectra for the formation of the long-lived excited state of $[Ru(bpy)_3)]^{2+}$ have been published (1–3). However,

- the spectral data above 500 nm have a poor signal-to-noise ratio;
- the spectrum has a very steep zero crossing near 270 nm, so that the differential absorption coefficient at 266 nm cannot be extracted accurately from the data published (1, 2);
- there was also some ambiguity with respect to the absolute scaling of the absorbance difference spectrum, with values ranging from -10 mM^{-1} cm^{-1} [ref. 3, recommended by IUPAC (4)] to -13.6 mM^{-1} cm^{-1} (2) at the visible absorption maximum of the ground state at 450 nm.

As the differential absorption coefficients at the laser wavelengths of our study are crucial for the evaluation of our transient absorption data on photorepair, we made an effort to determine these values accurately.

In order to improve the signal-to-noise ratio and to guarantee the same overlap between excitation and monitoring light beams at all wavelengths, the transient absorption setup described in *Materials and Methods* was modified as follows:

- The 266 nm monitoring beam was passed into the setup for the visible, and all polarization optics (which were of different optical material for 266 nm than for the visible) were taken out of the beam. Polarization doesn't matter on the nanosecond time scale studied here, because the rotational diffusion time of $[Ru(bpy)_3)]^{2+}$ in water at room temperature is approximately 150 ps (5).
- A $10 \times 2 \times 2$ mm (length × width × height) quartz cell with self-masking solid black walls and three clear windows (16.40-F/GL14/S/Q/10/Z15 from Starna) was used aerobically. Its position was unchanged throughout all experiments.
- All monitoring light beams where shaped such that their cross-section at the entrance of the cell exceeded the 2×2 mm window size, so that the entire inner volume was hit by the monitoring light.
- The excitation beam covered the entire 2×10 mm window of the cell at approximately 1.5 mJ/cm^2.

Relative absorption coefficients at 266, 448, 473, 488, 562, and 690 nm were obtained by comparison of the signal amplitudes of a 20 μM aqueous $Ru(bpy)_3Cl_2$ solution at these monitoring wavelengths. The absolute scaling was based on a differential absorption coefficient $\Delta\epsilon_{450} = -10$ mM^{-1} cm^{-1} (3, 4); the very minor difference in bleaching between 450 and 448 nm (2) was neglected.

Use of $[Ru(bpy)_3]^{2+}$ as Reference for the Quantification of Transient Absorption Data on Photolyase. We used the fast rising (<1 ps), long-lived (lifetime of several hundred ns) excited state of $[Ru(bpy)_3]^{2+}$ (6, 7) as a reference for the quantification of intermediates and the reaction product of CPD repair by photolyase. For each transient absorption experiment on photolyase, a reference experiment was performed on the ruthenium complex, at the same wavelength λ, in the same setup, and at identical geometry of sample, monitoring light beam, and excitation as for the photolyase experiment. The relation

$$\frac{\Delta A_i^{(\lambda)}(t)}{\Delta A_{Ru^*}^{(\lambda)}} = \frac{Y_i(t)\Delta\varepsilon_i^{(\lambda)} c_{PL}\varepsilon_{PL}^{exc}E_{PL}^{exc}}{Y_{Ru^*}\Delta\varepsilon_{Ru^*}^{(\lambda)} c_{Ru}\varepsilon_{Ru}^{exc}E_{Ru}^{exc}} \qquad \textbf{[S1]}$$

was used to calculate the (transient) population $Y_i(t)$ of a reaction intermediate (or product) i in the repair reaction from the accompanying transient absorbance change $\Delta A_i^{(\lambda)}(t)$, and vice versa. Population was defined as amount of intermediate (or product) at a given time per originally excited molecule. $\Delta\varepsilon_i^{(\lambda)}$ denotes the differential absorption coefficient for the formation of i. $\Delta A_{Ru^*}^{(\lambda)}$ is the absorbance change due to full formation of the long-lived excited state of the ruthenium complex; we obtained $\Delta A_{Ru^*}^{(\lambda)}$ by averaging the transient absorbance change in the time window from 2 to 6 ns. Y_{Ru^*} and $\Delta\varepsilon_{Ru^*}^{(\lambda)}$ are the corresponding population and differential absorption coefficient, respectively. c_{PL} and c_{Ru} denote the ground state concentrations of photolyase and ruthenium complex, respectively, prior to excitation, and ε_{PL}^{exc} and ε_{Ru}^{exc} the respective ground state absorption coefficients at the excitation wavelength (5.6 $mM^{-1}\,cm^{-1}$ (8) and 5.9 $mM^{-1}\,cm^{-1}$ (7), respectively, at 355 nm). E_{PL}^{exc} and E_{Ru}^{exc} are the measured excitation energies in the respective experiments. Ideally, they should be identical, but with our excitation laser, shot-to-shot variations in the order of a few percent were observed. As the quantum yield for formation of the long-lived excited state of $[Ru(bpy)_3]^{2+}$ is 100% (7), Y_{Ru^*} was set to 1.

Eq. **S1** also served to calculate differential absorption coefficients for the formation of $FADH^{-*}$ (Fig 2*A*) from transient absorption measurements on photolyase in the absence of substrate. A value of 1 was used for the population of $FADH^{-*}$ immediately after excitation.

It is of note that Eq. **S1** holds exactly only in the low excitation limit (no multiple excitations). We consider Eq. **S1** as a reasonable approximation for our experiments, as multiple excitations were not frequent (see estimation below), ε_{PL}^{exc} and ε_{Ru}^{exc} at 355 nm are very similar, and E_{PL}^{exc} and E_{Ru}^{exc} deviated by not more than a few percent for a given monitoring wavelength.

Evaluation of Flavin-Based Transient Absorbance Changes in the Visible. $FADH^{-*}$ can be monitored conveniently at 690 nm, as no other species in the photolyase-substrate system is expected to contribute significantly at this wavelength (see Fig. 2*A*). Both in the absence and in the presence of substrate, the absorbance at 690 nm rose instantaneously after the excitation flash (Fig. 2*B*), due to formation of $FADH^{-*}$. In the absence of substrate, the transient absorbance at 690 nm decayed with a time constant of 1.25 ns, in line with previous studies of the lifetime of $FADH^*$ in photolyase (9, 10) (a small, additional 200-ps component as previously reported (9) would not be resolvable in our setup). T = T present in the binding pocket is known to accelerate the decay of $FADH^{-*}$ into the 0.2 nanosecond range due to electron transfer from $FADH^{-*}$ to the T = T (9). Indeed, we observed a strong acceleration of the decay of the transient absorption at 690 nm upon addition of the substrate (Fig. 2*B*). The decrease of the apparent amplitude reflects the bandwidth limitation (1.7 GHz) of our setup. The signal in the presence of substrate contained a minor decay with kinetics similar to that of photolyase in the absence of substrate, presumably due to a fraction (approximately one third) of photolyases containing improperly bound substrate and/or improperly bound flavin. This fraction was ignored for the quantification of $FADH^\bullet$ formation and T = T repair per excited photolyase discussed in this work.

Formation of the flavin radical $FADH^\bullet$ is accompanied by marked absorption changes in the UV and visible spectral regions (see the $FADH^\bullet$-minus-$FADH^-$ difference spectrum shown as black line in Fig. 2*A*). In order to obtain the kinetics of $FADH^\bullet$ during photorepair, we monitored the transient absorbance changes of photolyase in the presence of substrate at 473 nm (red trace in Fig. 2*C*). Unfortunately, throughout the visible wavelength range, the excited state $FADH^{-*}$ contributes to the absorbance changes with an absorption coefficient similar to that of $FADH^\bullet$ (Fig. 2*A*). For recovering the true kinetics of $FADH^\bullet$ in the presence of substrate, we had to subtract the contribution of $FADH^{-*}$ from the measured signal. The contribution of $FADH^{-*}$ at 473 nm (black dotted trace in Fig. 2*C*) was obtained by rescaling the $FADH^{-*}$ kinetics observed at 690 nm in the presence of substrate (red trace in Fig. 2*B*) according to the amplitude ratio between the absorbance changes at 473 and 690 nm in the absence of substrate (blue traces in Fig. 2 *C* and *B*, respectively). Subtraction of the black dotted trace from the red trace in Fig. 2*C* yielded the true kinetics of $FADH^\bullet$ shown in Fig. 3*A* (noisy blue trace). The amplitude was converted from absorbance change to population ($FADH^\bullet$ per originally excited photolyase) by use of the $[Ru(bpy)_3]^{2+}$ signal at 473 nm as a reference (see above).

Similar to the experiments at 473 nm, we studied transient absorption changes at 488 and 562 nm in order to obtain the kinetics of $FADH^\bullet$ during photorepair experiments (Fig. S2). Compared to 473 nm, these wavelengths are less favorable because the contribution of $FADH^\bullet$ relative to $FADH^{-*}$ is weaker (see Fig. 2*A*) and hence the signal-to-noise ratio of the $FADH^\bullet$ kinetics deduced from the experimental data is poorer.

Determination of the $FADH^\bullet$-minus-$FADH^-$ Absorption Difference Spectrum in Photolyase in the UV. For deducing the T = T repair kinetics from transient absorption measurement at 266 nm, it is essential to know the contribution of formation and decay of $FADH^\bullet$ at this wavelength. MacFarlane and Stanley (11) reported that the $FADH^\bullet$-minus-$FADH^-$ difference spectrum in photolyase shows a strong negative peak around 255 nm, a strong positive one at approximately 275 nm, and a zero crossing at 267 ±2 nm. Based on these data, it would not be certain whether the absorbance change at 266 nm is positive or negative. We therefore set out to determine this difference spectrum more accurately. Photoreduction of $FADH^\bullet$ in photolyase by continuous light according to ref. 12 yielded the difference spectrum shown as solid line in Fig. 2*A* and Fig. S3*B*, with a zero crossing at 264.1 ±0.3 nm (span of six independent experiments). Comparison with the spectrum in ref. 11 (broken line in Fig. S3*B*) suggests a vertical offset as the main origin of the difference in zero crossing. In fact, these spectra are differences between two measurements recorded at a certain time interval (required for performing the photoreduction) in a spectral range where the protein absorbs much stronger than the flavin cofactor and where light scattering can be rather strong. In our case (solid line), the cell had to be taken out of the spectrometer for several minutes for photoreduction on ice. Minor changes in light scattering and protein absorption during the photoreduction treatment or differences in cleanness of the cell surfaces after wiping of water that condensed during photoreduction on ice might have caused a slight offset of the absorbance difference spectrum in the UV. We therefore developed a method to determine the zero crossing of the $FADH^\bullet$-minus-$FADH^-$ difference spectrum in photolyase more directly and accurately.

An anaerobic photolyase sample (2.5 μM $FADH^\bullet$) containing 1 mM cysteine as an extrinsic reductant was exposed to a series of

laser flashes at 532 nm that excited exclusively the neutral radical form $FADH^{\bullet}$ of the flavin cofactor and transformed part of it to $FADH^{-}$. Absorbance of the sample at several wavelengths close to the expected zero crossing was monitored in real time during such flash series. It was expected, that the absorbance would not change during the flash series at the zero crossing wavelength, whereas it should evolve with opposite sign at opposite sides of the zero crossing wavelength.

The setup was essentially as described in ref. 12, using a diode T9F26C (from Seoul Semiconductors) emitting up to 350 μW CW light at 265±7 nm (half height of the emission band) and a solar-blind photomultiplier R6834 (from Hamamatsu) for detection. Specific monitoring wavelengths were selected by tilting a narrow-band (2 nm FWHM) interference filter LL01-266 (from Semrock) that was placed between the light emitting diode and the sample. Monitoring light spectra were measured with a HR4000 fiber spectrometer (Ocean Optics) that had been calibrated by the 266 nm CW laser used for monitoring CPD repair. Excitation flashes [532 nm, 5 ns duration, approximately 2 mJ/cm^2 at the large window of the $10 \times 2 \times 8$ mm (length × width × height) cell, repetition rate 2 Hz] were provided by a Nd/YAG laser Brillant B (from Quantel).

After a series of flashes, the sample was gently shaken in order to dilute the excited volume (160 μl) into the total volume (240 μl), and an absorption spectrum was recorded, in order to quantify the amount of $FADH^{\bullet}$ that had been photoreduced, from comparison with a spectrum recorded prior to the flash series.

Fig. S3*A* shows the absorbance changes induced by the flash series observed at three selected wavelengths, including 263.7 nm, where virtually no effect occurred. As expected, absorbance increased below this wavelength because $FADH^{\bullet}$ absorbs less than $FADH^{-*}$, and vice versa above 263.7 nm. The difference between the absorption spectra measured before and after the flash series monitored at 266.0 nm is shown in the inset of Fig. S3*A*. This spectrum was used to calibrate the absorption change observed during the flash series assuming an $FADH^{\bullet}$ absorption coefficient of 5 $mM^{-1}\,cm^{-1}$ at 586 nm and taking into account the dilution of the excited volume. The same procedure was applied to all other wavelengths studied. The resulting $FADH^{\bullet}$-minus-$FADH^{-}$ differential absorption coefficients are presented as closed circles in Fig. S3*B*. The $FADH^{\bullet}$-minus-$FADH^{-}$ difference spectra obtained by photoreduction with continuous light by MacFarlane and Stanley (11) and by ourselves, both scaled to 5 $mM^{-1}\,cm^{-1}$ at 586 nm, are presented by broken and solid lines, respectively. Our data provide strong evidence that the zero crossing of the $FADH^{\bullet}$-minus-$FADH^{-}$ difference spectrum is very close to 264 nm. The differential absorption coefficient at 266.0 nm is 8.6 ± 1.5 $mM^{-1}\,cm^{-1}$ according to our flash method, and 7.0 ± 0.8 $mM^{-1}\,cm^{-1}$ from our photoreduction spectrum obtained by continuous illumination (Fig. S3*B*, solid line) and slightly up-shifted to fit with the data point at 263.7 nm obtained from the flash series. If the difference spectrum reported in ref. (11) (Fig. S3*B*, broken line) is up-shifted in the same way, one obtains 6.0 ± 0.8 $mM^{-1}\,cm^{-1}$ at 266 nm.

Extraction of the CPD Repair Kinetics from Transient Absorption Data. In addition to DNA-based reactions, formation and decay of the excited state $FADH^{-*}$ and of the semi-reduced flavin cofactor, $FADH^{\bullet}$, contribute to the absorbance changes at 266 nm. These flavin-based contributions were subtracted from the observed transient absorption signal at 266 nm as outlined below and illustrated in Fig. S4.

The $FADH^{-*}$ contribution at 266 nm was constructed essentially as described for 473 nm above, based on the 266 nm transient absorption signal observed in the absence of substrate (Fig. 2*D*, blue trace), and the quenching effect of substrate addition on the $FADH^{-*}$ kinetics observed at 690 nm (Fig. 2*B*, blue and red traces). However, we had to take into account that the (initially negative) 266 nm signal in the absence of substrate did not decay exactly to zero on the 7-ns time scale, but rather to a slightly positive value (approximately 5% of the total absorbance increase in the presence of substrate). The minor long-lived positive absorbance change in the absence of substrate can be explained by a small fraction of long-lived $FADH^{\bullet}$ that is formed due to electron ejection from $FADH^{-*}$ that occurs with low yield upon excitation by a second photon at 355 nm.

In fact, in order to obtain a reasonable signal-to-noise ratio in the measurements at 266 nm [where only a low photolyase concentration (approximately 4 μM) could be used because of the strong absorption of the protein], we had to apply a considerably higher excitation energy (approximately 10 mJ/cm^2) than for the experiments in the visible (approximately 1 mJ/cm^2) where the photolyase concentration was in the order of 40 μM. At 10 mJ/cm^2, the probability that $FADH^{*}$ absorbs more than one photon is approximately 6% (for this rough estimation, we assumed that $FADH^{-*}$ absorbs as well as $FADH^{-}$ at 355 nm), at 1 mJ/cm^2, this probability is only approximately 0.08%.

In order to verify this explanation for the long-lived absorption increase at 266 nm in the absence of substrate, we searched for formation of hydrated electrons e^{-}_{aq} at the higher excitation energy. Fig. S5 shows transient absorption traces at 690 nm, where e^{-}_{aq} has strong absorption (approximately 23.5 $mM^{-1}\,cm^{-1}$) (13), at 9 mJ/cm^2 (black) and 0.6 mJ/cm^2 (red, x15) excitation energy for a photolyase sample containing no substrate. These data clearly show the presence of a long-lived species only at high excitation energy, as expected for formation of hydrated electrons by multiple excitations. The amplitude of the signal at 5 ns after excitation with 9 mJ/cm^2 is consistent with the formation of approximately 0.01 e^{-}_{aq} per photolyase. One would expect approximately the same yield of long-lived $FADH^{\bullet}$, i.e., approximately 37 nM in the 3.7 μM photolyase sample of the 266-nm experiments (for the same excitation energy, and approximately 50% more at the 11.6 mJ/cm^2 applied for the experiment shown in Fig. 2*D*), which is consistent with the observed long-lived absorbance increase assuming a $FADH^{\bullet}$-minus-$FADH^{-}$ differential absorption coefficient of 7 $mM^{-1}\,cm^{-1}$ at 266 nm (see above). The absorption of e^{-}_{aq} at 266 nm is very weak (0.6 $mM^{-1}\,cm^{-1}$) (14).

As electron ejection from doubly excited $FADH^{-}$ should be immediate, we modeled the contribution of $FADH^{\bullet}$ formed by this process to the transient absorbance changes at 266 nm by downscaling the signal measured with the $Ru(bpy)_3Cl_2$ solution (green trace in Fig. 2*D*) to the asymptotic amplitude of the signal for photolyase without substrate (blue trace in Fig. 2*D*). The resulting trace for the long-lived $FADH^{\bullet}$ contribution (dashed olive trace in Fig. S4) was subtracted from the measured signal for photolyase without substrate. The resulting solid blue trace in Fig. S4 should represent the true contribution of $FADH^{-*}$ at 266 nm in the absence of substrate and was used to construct the contribution of $FADH^{-*}$ in the presence of substrate (dashed magenta trace in Fig. S4) as done for 473 nm (see above).

The contribution at 266 nm of $FADH^{\bullet}$ decaying within a few ns (dashed purple trace in Fig. S4) was obtained by proper scaling of its population kinetics (noisy blue trace in Fig. 3*A*) with respect to the signal measured at 266 nm with the $Ru(bpy)_3Cl_2$ solution, using Eq. **S1** with a $FADH^{\bullet}$-minus-$FADH^{-}$ differential absorption coefficient of 7 $mM^{-1}\,cm^{-1}$ at 266 nm. Finally the contributions of $FADH^{-*}$, transient $FADH^{\bullet}$ and long-lived $FADH^{\bullet}$ were subtracted from the trace measured in the presence of substrate to obtain the DNA-based contribution (solid black trace in Fig. S4). The latter was converted to a population scale (red trace in Fig. 3*A*) using Eq. **S1** with a differential absorption coefficient for T = T repair of 18.4 $mM^{-1}\,cm^{-1}$ at 266 nm (12).

Solution of the Kinetic Scheme and Convolution with the Instrument Response Function. The kinetic scheme in Fig 3*B* is described by the following system of differential equations, where upper case letters signify the (transient) population of the corresponding state (amount present at time t per originally excited photolyase), and the prime signifies the time derivative:

$$A' = -(k_{\text{et}} + k_d)A(t)$$

$$B' = k_{\text{et}}A(t) - (k_{\text{split}} + k_{\text{rec}})B(t)$$

$$C' = k_{\text{split}}B(t) - k_{\text{er}}C(t)$$

$$P' = k_{\text{er}}C(t)$$

$$R' = k_dA(t) + k_{\text{rec}}B(t)$$

Initially, only state A (excited reduced flavin) is populated (nonexcited flavin was ignored):

$$A(t=0) = 1;$$
$$B(t=0) = C(t=0) = P(t=0) = R(t=0) = 0$$

This system has for general solution a sum of three exponentials and a constant:

$$X(t) = X0 + X1\exp(-t/\tau 1) + X2\exp(-t/\tau 2) + X3\exp(-t/\tau 3) \quad \textbf{[S2]}$$

where X is any of A, B, C, and P.

$$R(t) = 1 - A(t) - B(t) - C(t) - P(t)$$

The three decay time constants τi are given by:

$$\tau 1 = 1/(k_{\text{et}} + k_d); \qquad \tau 2 = 1/(k_{\text{split}} + k_{\text{rec}}); \qquad \tau 3 = 1/k_{\text{er}}$$

The amplitudes Xi in Eq. **S2** are given by:

$$A0 = 0;$$

$$A1 = 1;$$

$$A2 = 0;$$

$$A3 = 0;$$

$$B0 = 0;$$

$$B1 = -k_{\text{et}}/(k_{\text{et}} - k_{\text{split}} - k_{\text{rec}} + k_d);$$

$$B2 = k_{\text{et}}/(k_{\text{et}} - k_{\text{split}} - k_{\text{rec}} + k_d);$$

$$B3 = 0;$$

$$C0 = 0;$$

$$C1 = k_{\text{et}}k_{\text{split}}/((k_{\text{et}} - k_{\text{er}} + k_d)(k_{\text{et}} - k_{\text{split}} - k_{\text{rec}} + k_d));$$

$$C2 = -k_{\text{et}}k_{\text{split}}/((k_{\text{split}} - k_{\text{er}} + k_{\text{rec}})(k_{\text{et}} - k_{\text{split}} - k_{\text{rec}} + k_d));$$

$$C3 = k_{\text{et}}k_{\text{split}}/((k_{\text{split}} - k_{\text{er}} + k_{\text{rec}})(k_{\text{et}} - k_{\text{er}} + k_d));$$

$$P0 = k_{\text{et}}k_{\text{split}}/((k_{\text{et}} + k_d)(k_{\text{split}} + k_{\text{rec}}));$$

$$P1 = -k_{\text{et}}k_{\text{split}}k_{\text{er}}/((k_{\text{et}} + k_d)(k_{\text{et}} - k_{\text{er}} + k_d)(k_{\text{et}} - k_{\text{split}} - k_{\text{rec}} + k_d));$$

$$P2 = k_{\text{et}}k_{\text{split}}k_{\text{er}}/((k_{\text{split}} + k_{\text{rec}})(k_{\text{split}} - k_{\text{er}} + k_{\text{rec}})(k_{\text{et}} - k_{\text{split}} - k_{\text{rec}} + k_d));$$

$$P3 = -k_{\text{et}}k_{\text{split}}/((k_{\text{split}} - k_{\text{er}} + k_{\text{rec}})(k_{\text{et}} - k_{\text{er}} + k_d))$$

The kinetic description of the populations of FADH° and of repaired T = T (restored thymine pairs) is obtained by:

$$\text{FADH}^\circ(t) = B(t) + C(t);$$

$$\text{CPD}_{\text{rep}}(t) = C(t)/2 + P(t)$$

These model kinetics are thus entirely defined by the five rate constants of the kinetic scheme.

For comparison with the experimental kinetics, the model kinetics were numerically convoluted (using the Origin8 "conv" routine, OriginLab) with the normalized instrument response function (see Fig. S6). The five rate constants were iteratively varied in order to obtain an optimal fit.

1. Miedlar K, Das PK (1982) Tris(2,2′-bipyridine)ruthenium(II)-sensitized photooxidation of phenols. Environmental effects on electron transfer yields and kinetics. *J Am Chem Soc* 104:7462–7469.
2. Lachish U, Infelta PP, Grätzel M (1979) Optical absorption spectrum of excited ruthenium tris-bipyridyl ($Ru(bpy)_3^{2+}$). *Chem Phys Lett* 62:317–319.
3. Yoshimura A, Hoffman MZ, Sun H (1993) An evaluation of the excited-state absorption-spectrum of $Ru(bpy)_3^{2+}$ in aqueous and acetonitrile solutions. *J Photochem Photobiol A Chem* 70:29–33.
4. Kuhn HJ, Braslavsky SE, Schmidt R (2004) Chemical actinometry (IUPAC Technical Report). *Pure Appl Chem* 76:2105–2146.
5. Malone RA, Kelley DF (1991) Interligand electron transfer and transition state dynamics in Ru(II)trisbipyridine. *J Chem Phys* 95:8970–8976.
6. Damrauer NH, et al. (1997) Femtosecond dynamics of excited-state evolution in $[Ru(bpy)_3]^{2+}$. *Science* 275:54–57.
7. Kalyanasundaram K (1982) Photophysics, photochemistry and solar energy conversion with tris(bipyridyl)ruthenium(II) and its analogues. *Coord Chem Rev* 46:159–244.
8. Jorns MS, Wang BY, Jordan SP, Chanderkar LP (1990) Chromophore function and interaction in *Escherichia coli* DNA photolyase: Reconstitution of the apoenzyme with pterin and/or flavin derivatives. *Biochemistry* 29:552–561.
9. Kao YT, Saxena C, Wang L, Sancar A, Zhong D (2005) Direct observation of thymine dimer repair in DNA by photolyase. *Proc Natl Acad Sci USA* 102:16128–16132.
10. Okamura T, et al. (1991) Picosecond laser photolysis studies on the photorepair of pyrimidine dimers by DNA photolyase. 1. Laser photolysis of photolyase-2-deoxyuridine dinucleotide photodimer complex. *J Am Chem Soc* 113:3143–3145.
11. MacFarlane AW, Stanley RJ (2003) *Cis-syn* thymidine dimer repair by DNA photolyase in real time. *Biochemistry* 42:8558–8568.
12. Thiagarajan V, et al. (2010) DNA repair by photolyase: A novel substrate with low background absorption around 265 nm for transient absorption studies in the UV. *Biochemistry* 49:297–303.
13. Hare PM, Price EA, Bartels DM (2008) Hydrated electron excitation coefficient revisited. *J Phys Chem A* 112:6800–6802.
14. Fielden EM, Hart EJ (1967) Activation energy of the hydrated electron + water reaction and the ultraviolet absorption spectrum of the hydrated electron. *Transactions of the Faraday Society* 63:2975–2982.

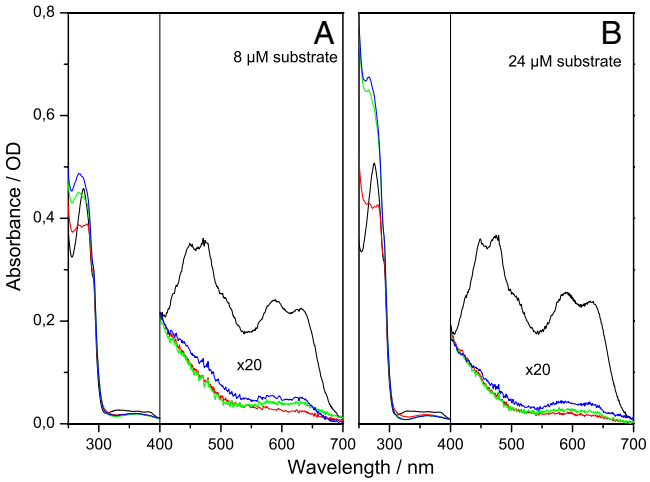

Fig. S1. Spectral characterization of sample preparation and repair reaction. Steady state absorption spectra were recorded for two samples with different substrate excess. Black lines, before photoreduction. Red lines, after photoreduction. Green lines, after substrate addition (4% of final volume). Blue lines, after transient absorption repair experiments at 266 nm. (*A*) 8 µM substrate; 2.9 µM photolyase (after substrate addition); 61 photorepairing flashes of 1.16 mJ mean energy at 355 nm were applied during transient absorption experiments. (*B*) 24 µM substrate; 3.2 µM photolyase; 46 flashes of 1.05 mJ mean energy. The optical path was 10 mm for all spectra. The 400–700 nm regions were upscaled by a factor of 20.

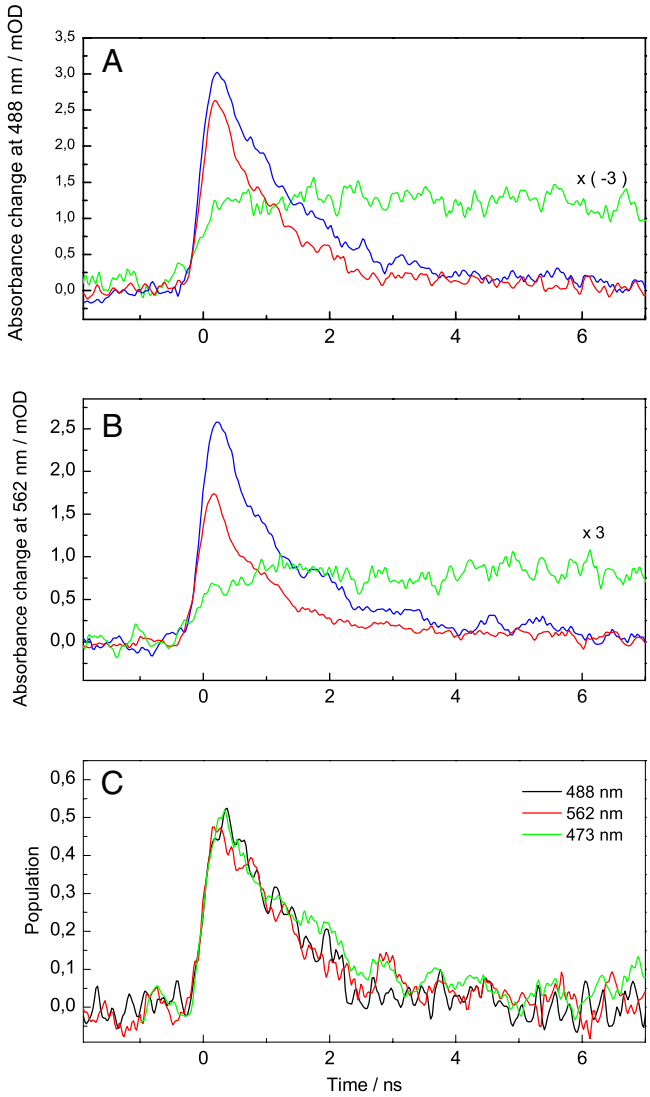

Fig. S2. FADH$^{\bullet}$ population kinetics obtained from transient absorption data at 488 and 562 nm. (*A* and *B*) Transient absorption data at 488 and 562 nm, respectively. Blue traces, photolyase without substrate. Red traces, photolyase with substrate. Green traces, aqueous solution of $Ru(bpy)_3Cl_2$ (21 μM). Photolyase concentration, 35 μM, excitation energy, 0.6 mJ/cm^2. Other details as for Fig. 2*C*. (*C*) Black and red traces, kinetics of the population of FADH$^{\bullet}$ (amount per originally excited photolyase) deduced from the experimental data at 488 and 562 nm, respectively, as described in *SI Text* for 473 nm. Green trace, FADH$^{\bullet}$ population kinetics deduced from 473 nm data (taken from Fig. 3*A*).

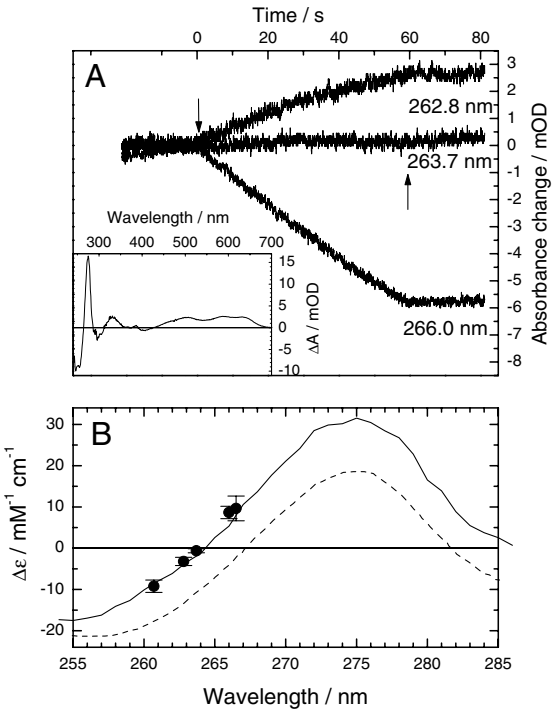

Fig. S3. Determination of the FADH$^{\bullet}$ minus FADH^{-} absorbance difference spectrum in the UV. (*A*) Absorbance changes induced by a series of laser flashes at 532 nm (start and end indicated by arrows). Inset: Difference (before minus after) between the absorption spectra measured before and after the flash series monitored at 266.0 nm. (*B*) Spectral data deduced from *A* (circles) and from photoreduction by CW light done by ourselves (solid line) and reported by MacFarlane and Stanley (11) (dotted line). See *SI Text* for details.

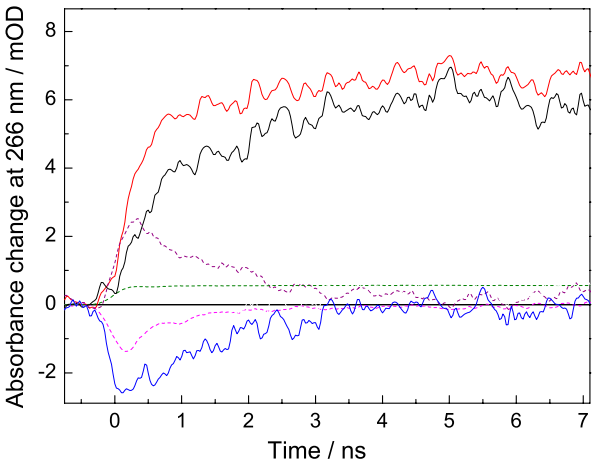

Fig. S4. Extraction of T = T repair kinetics from transient absorption data. The black solid trace describing the 266 nm absorbance increase due to formation of intact thymines by T = T repair was obtained from the experimental data in the presence of substrate (red solid trace, taken from Fig. 2*D*) by subtraction of the three FAD-based contributions represented by the dashed traces. Blue solid trace, Experimental data in the absence of substrate (from Fig. 2*D*), corrected for a small long-lived contribution from FADH$^{\bullet}$ (olive dashed trace) due to electron ejection from excited FADH^{-} (see *SI Text*). Purple dashed trace, contribution from FADH$^{\bullet}$ formation and decay deduced from 473 nm data (Fig. 2*C* and blue noisy trace in Fig. 3*A*) and scaled to absorption units at 266 nm by Eq. **S1**. Magenta dashed trace, contribution from the excited state of FADH^{-} in the presence of substrate as observed at 690 nm and scaled to 266 nm as described in the *SI Text*).

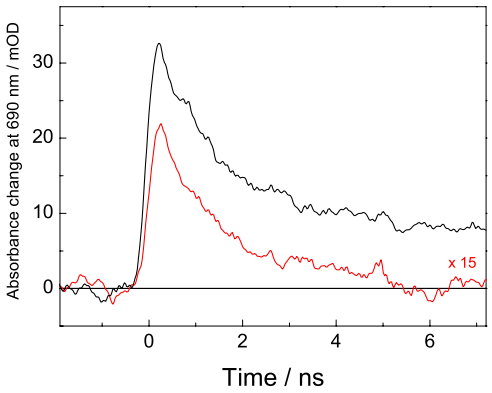

Fig. S5. Indication for hydrated electron formation by multiple photon absorption at high excitation density. Absorbance changes at 690 nm were recorded for photoreduced photolyase (37 μM) in the absence of substrate upon excitation with 355 nm flashes of 0.6 mJ/cm^2 (red, 15-fold magnified) or 9 mJ/cm^2 (black).

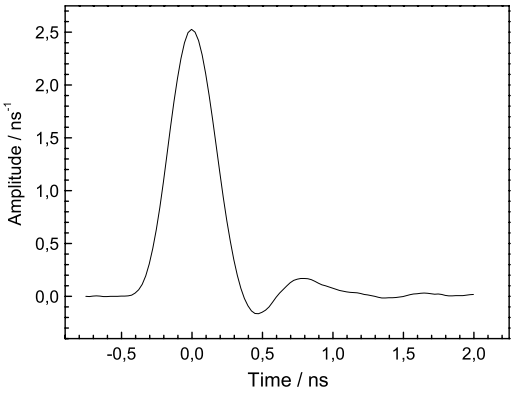

Fig. S6. Instrument response function of the transient absorption setup used in this study to detect enzymatic photorepair. Excitation flashes at 355 nm were attenuated and scattered onto the photodiode. 128 signals were averaged. The amplitude was scaled to yield an integrated area of 1.